Conformational effects of UV light on DNA origami

JACS
JOURNAL OF THE AMERICAN CHEMICAL SOCIETY

Communication

pubs.acs.org/JACS

Conformational Effects of UV Light on DNA Origami

Haorong Chen,[†] Ruixin Li,[†] Shiming Li,[‡] Joakim Andréasson,[‡] and Jong Hyun Choi*[,†]

[†]School of Mechanical Engineering, Purdue University, West Lafayette, Indiana 47907, United States

[‡]Department of Chemistry and Chemical Engineering, Chalmers University of Technology, SE-412 96 Gothenburg, Sweden

Supporting Information

ABSTRACT: The responses of DNA origami conformation to UV radiation of different wavelengths and doses are investigated. Short- and medium-wavelength UV light can cause photo-lesions in DNA origami. At moderate doses, the lesions do not cause any visible defects in the origami, nor do they significantly affect the hybridization capability. Instead, they help relieve the internal stress in the origami structure and restore it to the designed conformation. At high doses, staple dissociation increases which causes structural disintegration. Long-wavelength UV does not show any effect on origami conformation by itself. We show that this UV range can be used in conjunction with photoactive molecules for photo-reconfiguration, while avoiding any damage to the DNA structures.

DNA origami has emerged as an important research tool because of its ability to form nanostructures of complex geometric designs.[1] The accurate spatial control, combined with a variety of chemical functionalizations to DNA,[2] has facilitated controlled organization of functional components such as proteins and nanoparticles. The precise positioning leads to novel properties and functions, such as increased catalytic activity of enzyme cascades[3,4] and chiral plasmonic coupling between gold nanoparticles.[5,6] There also have been continuous efforts in the dynamic control of DNA origami conformation. Such ability adds a temporal dimension to the impressive spatial control of DNA origami. As the origami changes its conformation in response to environmental cues or external signals, the attached functional components are reorganized, leading to a modulation of the functional properties. Therefore, conformation change of DNA origami can lead to the development of new sensors and actuators at the nanoscale. Such examples include an origami pincer that closes itself on its analyte[7] and 3D origami boxes that opens up to expose its drug payload in response to a combination of physiological signals.[8,9]

Among the various mechanisms demonstrated to date, photonic control of origami conformation is especially powerful.[10,11] Azobenzene moieties has been covalently incorporated into designated DNA strands.[12] The photoisomerization between *trans* and *cis* forms leads to the hybridization and dissociation of the host DNA, eventually switching the origami between locked and relaxed conformations.[10] Besides azobenzene, a variety of photo-labile and photochromic groups (e.g., photo-cleavable linkers and spiropyran) can also be used to render DNA origami photoresponsive[13,14] However, the action spectra of many of the moieties are in the ultraviolet (UV) range, which poses a potential issue since DNA can absorb UV light and undergo unwanted photochemical changes. Such changes may affect the conformation/function of DNA origami structures, and therefore, need to be examined for a good understanding and proper execution of photonic control.

In this communication, we have explored the conformational effects of UV light and demonstrated the "flattening" effect of short- and medium-wavelength UV radiation (UVC and UVB, respectively). The internal stress in origami was relieved by the minor lesions induced by the UV light, resulting in as-designed flat conformation. The effects by various UV wavelengths and at higher radiation doses were also studied. Long-wavelength UV light (UVA) was found to have minimal conformational effect on DNA origami and thus can be used to stimulate photoactive chemical moieties, while avoiding side effects caused by direct changes of DNA. As a demonstration, we used this wavelength range to activate a DNA intercalator that can subsequently switch the conformation of DNA origami.

Two types of DNA origami were used as model systems to examine their responses to UV radiation. The schematics are illustrated in Figure 1a,d (design details are presented in the Supporting Information). Both structures are designed with caDNAno by using the square lattice framework,[15] which assumes that B-form DNA double helices make three full turns every 32 base-pairs (10.67 bp/turn). In contrast, the relaxed helicity of B-form DNA is 10.4−10.5 bp/turn.[16−18] The difference causes DNA helices in the origami to be slightly underwound and generates internal stress in both structures. The first design is a single-layer structure consisting of 32 DNA duplexes connected in parallel. Although the structure was designed to be a flat rectangle, the internal stress causes it to curve up, as shown by finite element method (FEM) CanDo simulation[19,20] in Figure 1a. The curvature can be more clearly observed experimentally when the rectangles are connected laterally into elongated ribbons, since the distortion of individual rectangles are accumulated into significant right handed twist. The dense parallelgram-shaped kinks along the ribbons in AFM images (Figures 1b, S4a, and S5a) indicate heavy twists in the ribbons. A close examination of the kink shape confirmed that the twist is indeed right-handed.[21]

Interestingly, a moderate dose of UV radiation can effectively suppress the distortion without causing any visible defects to the origami structures. This is likely achieved by relieving the internal stress. Since the structures are restored to their

Received: October 24, 2016
Published: January 17, 2017

DOI: 10.1021/jacs.6b10821
J. Am. Chem. Soc. 2017, 139, 1380−1383

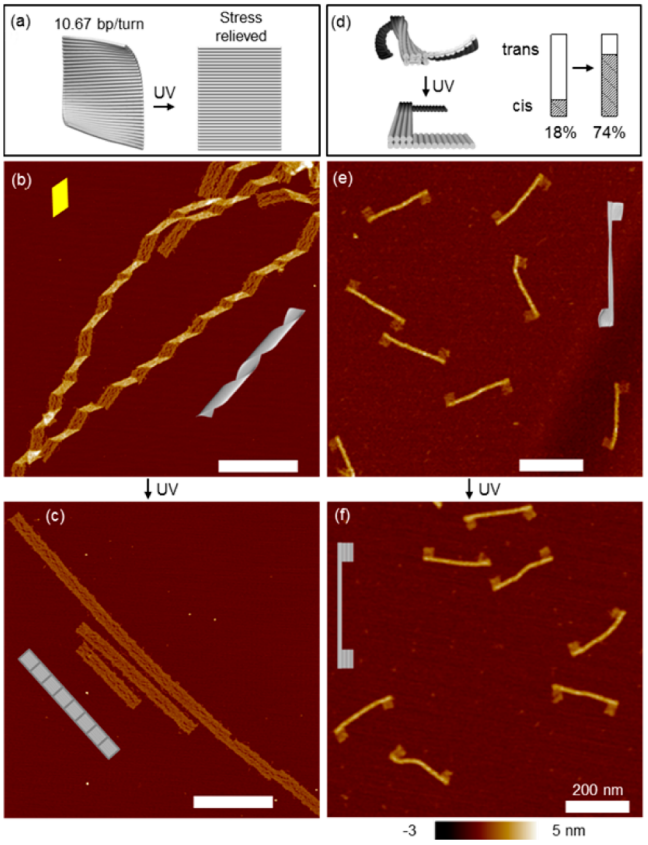

Figure 1. Flattening effect of UV radiation on DNA origami. (a) Schematic of an origami rectangle. While it is designed to be flat, internal stress causes it to curve up. Moderate UV radiation changes it back to the designed flat conformation. (b) AFM image of ribbons polymerized from curved origami rectangles. The curvature of the tiles causes the ribbon to twist heavily. The yellow parallelogram highlights the shape of the kinks, which can be used to identify the right-handed twist. (c) AFM image of UVC-irradiated ribbons (~2.5 kJ/m^2), which are completely flattened. (d) Schematic of an origami shaft. The shaft is designed to be in a *cis*-form, but twists to a *trans*-form under intrinsic conditions due to internal stress. UV radiation relieves the stress and reverts the conformation to a *cis*-form. (e,f) AFM images of the shaft (e) before and (f) after UV radiation. The majority of *trans*-form shafts are shifted to the *cis*-form after UVC irradiation (~2.5 kJ/m^2).

designed flat conformation, we term it the "flattening" effect. As shown in Figures 1c, S4d, and S5b, the ribbons seldom exhibit any twist. Even micrometer-long ribbons are deposited perfectly flat. Among the three wavelengths that we tested (366, 312, and 254 nm which roughly correspond to UVA, UVB, and UVC), 254 and 312 nm were quite effective at flattening, while 366 nm did not cause any significant change (*vide infra*). With increasing dose, the degree of twisting was gradually reduced (Figure S4). Eventually, the ribbons became completely flattened after a sufficient dose was applied, which we term the "flattening dose".

The flattening effect can be similarly demonstrated with a second origami model system. As shown in Figure 1d, eight DNA double helices are bundled in a square lattice to form an origami shaft structure. Each end of the shaft has a flag attached for displaying the twisting state of the shaft. While the flags were designed to be on the same side (*cis*-form), the internal stress causes the shaft to twist about 180°, as shown by FEM simulation. Correspondingly, the two flags would be placed on opposite sides of the shaft (*trans*-form), as confirmed by AFM (Figure 1e). Upon UV irradiation, the stress relief changes the majority of origami back to *cis*-form, as shown by the AFM image in Figure 1f and the statistics in Figure 1d.

The flattening effect is likely due to the sporadic lesions in the origami. Cyclobutane pyrimidine dimer (CPD) is known to be the most frequent type of DNA lesions generated by UV light in the absence of photosensitizers[22−24] As shown in Figure S6, generation of CPD in UV irradiated origami can be confirmed by visualizing the binding of photolyase, a DNA repair enzyme that specifically bind to CPD.[25,26] At the CPD site, the covalent linkage between neighboring pyrimidines disrupts the base-stacking within a single stand and the base-pairing between complementary strands, destabilizing the mechanical reinforcement between the two strands.[27,28] Conseqeuntly, the DNA duplex should be much more flexible at the lesion site and can easily deform to relieve the internal stresses. Meanwhile, the intact flanking regions still ensure the correct binding of the staples and maintain the structural integrity of the origami.

The flattening effect of UV radiation can be useful for DNA nanotechnology. Since duplexes in DNA origami are made up by a discrete number of base-pairs, the distance between crossovers cannot be continuously tuned to fit the most relaxed helicity. As a result, internal stress is common, and its relief should be useful for controlling the conformation (and funcional properties) of DNA origami.[29] UV irradiation is a straightforward method that avoids introducing foreign chemicals for such purpose. We have also confirmed that the moderate UV dose for flattening does not significantly affect the hybridization ability of DNA origami, hence it would not compromise its function of organizing other chemical groups. Origami rectangles exposed to the flattening dose were mixed with linkers and incubated at 37 °C following the same protocol as unexposed ones. The exposed tiles successfully hybridized with the linkers and connected into flat ribbons whose lengths are comparable with their unexposed counterpart (Figure S7). As a further validation, the exposed origami could also be reannealed into intact rectangles with high yield after being thermally denatured into scaffold and staple (Figure S8).

Excessive UVB and UVC radiation can cause severe damage to DNA origami. As shown in Figure 2a, visible defects became evident at high doses. They are mostly holes caused by failed connection between adjacent duplexes. The increasing photolesion density destabilized the hybridization between staples and the scaffold, causing the failed connection. At even higher doses, the structures were completely destroyed and only irregular fragments could be found (Figure 2c). Agarose gel electrophoresis was used to monitor the fragmentation of origami. Figure 2d shows a gel image of origami samples after receiving various UVC doses. The intensity of the distinct bands can be used to quantify the amount of origami tiles that still retain their original size. The quantified data are presented in Figure 2e. The band intensity maintains constant up to a dose and then decreases dramatically. AFM confirms that the onset of intensity drop coincides with origami fragmentation (Figure 2b). The doses for causing various conformation effects are summarized in Table 1. The internal stresses are sufficiently relieved at flattening doses. The further accumulation of lesions causes visible defects at about 3 times the flattening dose. Structure fragmentation becomes significant at about 6 times the flattening dose.

DOI: 10.1021/jacs.6b10821
J. Am. Chem. Soc. 2017, 139, 1380−1383

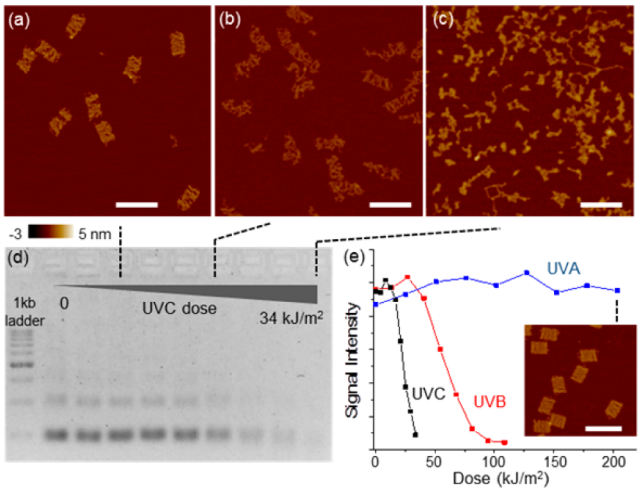

Figure 2. (a–c) AFM images of DNA origami tiles after various doses of UVC radiation. (d) Agarose gel image of UVC-irradiated origami samples. (e) Band intensity as a function of UV dose. The band intensities start to drop sharply after enough doses of UVC and UVB. No significant intensity drop or visible damage in AFM was observed after UVA irradiation. Scale bar: 200 nm.

Table 1. Threshold Dose for Different Conformational Effects

	dose (kJ/m^2) for causing:		
UV source	flattening	visible defect	fragmentation
UVC	2.5	8.3	16.7
UVB	6.8	20.3	40.6

It is noteworthy that the UVA source used in this study (centered at 366 nm) did not cause any visible damages even at a high dose (AFM image in Figure 2e), nor did it induce any significant flattening effect. As shown later in Figure 3, the heavily UVA irradiated origami ribbons were still highly twisted at a similar density as before. Scaffolds exposed to high doses of UVA (e.g., ~200 kJ/m^2) were also observed to fold into correct origami with high yield (Figure S10). These results indicate that the conformational effect of UVA is very weak, in agreement with other reports in the literature.[22] Because DNA origami has minimal conformational response to UVA, this wavelength is ideal for the light-control of DNA origami using photo-sensitive molecules. As side effects on DNA can be practically ignored, the design for photo-reconfiguration of DNA origami may be greatly simplified.

With UVA, we demonstrated light-control of DNA origami conformation by activating a photo-responsive molecule. As illustrated in Figure 3a, a triarylpyridinium cation (TP1) can be biscyclized into a polycyclic form (TP2) by UVA radiation. The photo-conversion can be monitored optically through the emergence of an absorption peak at 432 nm (Scheme S1). While TP1 does not interact strongly with DNA, TP2 is a DNA intercalator with a dissociation constant K_D of ~1.7 μM.[30] As anticipated, the origami ribbon conformation was not significantly affected by the addition of TP1 or by UVA radiation alone (Figure 3b,c). In contrast, UVA radiation in the presence of 8.5 μM TP1 significantly changed the twisting state of the origami. The ribbons became largely flattened at a dose of ~25 kJ/m^2 (Figure 3d). At a higher dose (~33 kJ/m^2), more TP1 molecules were converted into the intercalating form which overcompensated the original stress (Figure 3e). The

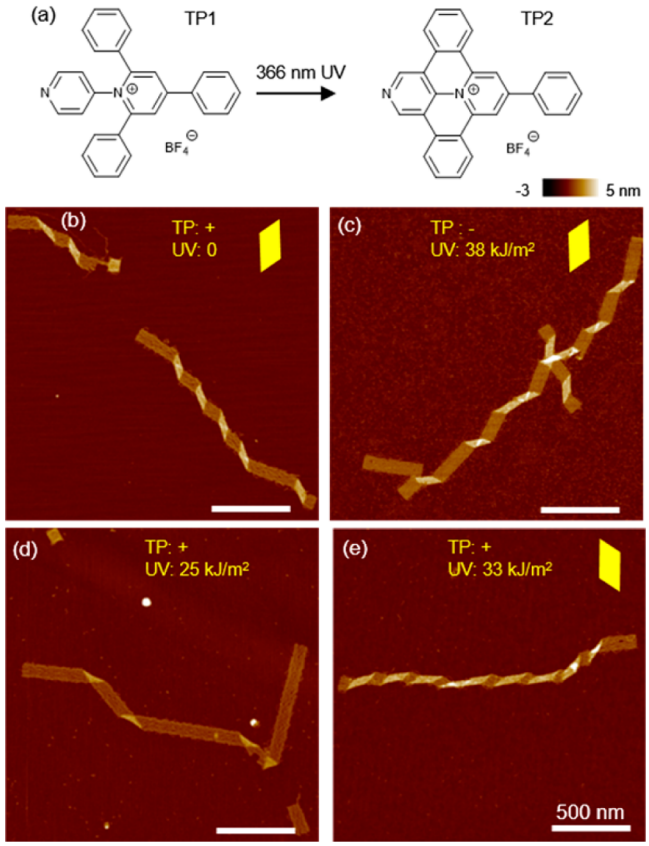

Figure 3. (a) Chemical structure of the triarylpyridinium (TP1) and its photo-product (TP2). TP1 does not interact with DNA, while TP2 is a DNA intercalator. TP1 can be converted to TP2 by UVA. (b–e) AFM images of origami ribbons under different combinations of TP addition and UVA radiation. (d,e) Conformation change occurs only when TP1 and UVA are both present. Partial activation leads to flattening (d), while full activation leads to a flip of twist handedness due to overcompensation (e). Yellow parallelogram highlights the kink shapes, indicating twist-handedness.

opposite stress forced the ribbons to flip their twist direction, as indicated by the flipped kink shapes in Figure 3e.[21] Thus, the drastic reversal of twist direction and the negative results in the control experiments confirm the feasibility to use UVA and photoactive molecules to control DNA origami, while avoiding photo-damage.

In summary, we have investigated the conformational effects of UV exposure to DNA origami. Radiation of short-wavelength (UVB and UVC) can directly affect the conformation of DNA origami. At a moderate dose, they suppress the deformation in the origami structure by relieving the internal stresses, while preserving the structural integrity and the hybridization capability of binding sites. Such flattening effect may be useful in tuning the conformation and mechanical property of DNA origami structures. The long-wavelength UVA radiation does not produce any conformational effect on its own. Therefore, it can be used as an ideal light source for switching photoactive molecules without side effects on DNA. By choosing suitable wavelength and light-sensitive molecules, UV radiation can be used as a flexible tool for dynamic DNA origami.

DOI: 10.1021/jacs.6b10821
J. Am. Chem. Soc. 2017, 139, 1380–1383

■ ASSOCIATED CONTENT

Supporting Information

The Supporting Information is available free of charge on the ACS Publications website at DOI: 10.1021/jacs.6b10821.

Experimental, analytical, and calculation details; AFM and gel images; and origami sequence information, including Tables S1 and S2, Scheme S1, and Figures S1–S15 (PDF)

■ AUTHOR INFORMATION

Corresponding Author

*jchoi@purdue.edu

ORCID

Haorong Chen: 0000-0002-8218-9817

Ruixin Li: 0000-0002-9079-1138

Jong Hyun Choi: 0000-0002-0507-3052

Notes

The authors declare no competing financial interest.

■ ACKNOWLEDGMENTS

This work was supported by the U.S. National Science Foundation (awards nos. 1334088, 1437301, and 1512537) and Office of Naval Research (awards nos. N00014-15-1-2707 and N00014-12-1-0829). Funding from the Swedish Research Council VR (VR 2016-03601) is also gratefully acknowledged.

■ REFERENCES

(1) Rothemund, P. W. *Nature* **2006**, *440*, 297.

(2) Endo, M.; Sugiyama, H. *ChemBioChem* **2009**, *10*, 2420.

(3) Linko, V.; Eerikäinen, M.; Kostiainen, M. A. *Chem. Commun.* **2015**, *51*, 5351.

(4) Fu, Y.; Zeng, D.; Chao, J.; Jin, Y.; Zhang, Z.; Liu, H.; Li, D.; Ma, H.; Huang, Q.; Gothelf, K. V.; et al. *J. Am. Chem. Soc.* **2013**, *135*, 696.

(5) Kuzyk, A.; Schreiber, R.; Fan, Z.; Pardatscher, G.; Roller, E.-M.; Högele, A.; Simmel, F. C.; Govorov, A. O.; Liedl, T. *Nature* **2012**, *483*, 311.

(6) Kuzyk, A.; Schreiber, R.; Zhang, H.; Govorov, A. O.; Liedl, T.; Liu, N. *Nat. Mater.* **2014**, *13*, 862.

(7) Kuzuya, A.; Sakai, Y.; Yamazaki, T.; Xu, Y.; Komiyama, M. *Nat. Commun.* **2011**, *2*, 449.

(8) Douglas, S. M.; Bachelet, I.; Church, G. M. *Science* **2012**, *335*, 831.

(9) Andersen, E. S.; Dong, M.; Nielsen, M. M.; Jahn, K.; Subramani, R.; Mamdouh, W.; Golas, M. M.; Sander, B.; Stark, H.; Oliveira, C. L.; et al. *Nature* **2009**, *459*, 73.

(10) Kuzyk, A.; Yang, Y.; Duan, X.; Stoll, S.; Govorov, A. O.; Sugiyama, H.; Endo, M.; Liu, N. *Nat. Commun.* **2016**, *7*, 10591.

(11) Yang, Y.; Endo, M.; Hidaka, K.; Sugiyama, H. *J. Am. Chem. Soc.* **2012**, *134*, 20645.

(12) Asanuma, H.; Liang, X.; Nishioka, H.; Matsunaga, D.; Liu, M.; Komiyama, M. *Nature protocols* **2007**, *2*, 203.

(13) Li, F.; Chen, H.; Pan, J.; Cha, T.-G.; Medintz, I. L.; Choi, J. H. *Chem. Commun.* **2016**, *52*, 8369.

(14) Andersson, J.; Li, S.; Lincoln, P.; Andréasson, J. *J. Am. Chem. Soc.* **2008**, *130*, 11836.

(15) Ke, Y.; Douglas, S. M.; Liu, M.; Sharma, J.; Cheng, A.; Leung, A.; Liu, Y.; Shih, W. M.; Yan, H. *J. Am. Chem. Soc.* **2009**, *131*, 15903.

(16) Dietz, H.; Douglas, S. M.; Shih, W. M. *Science* **2009**, *325*, 725.

(17) Li, Z.; Wang, L.; Yan, H.; Liu, Y. *Langmuir* **2012**, *28*, 1959.

(18) Woo, S.; Rothemund, P. W. *Nat. Chem.* **2011**, *3*, 620.

(19) Castro, C. E.; Kilchherr, F.; Kim, D.-N.; Shiao, E. L.; Wauer, T.; Wortmann, P.; Bathe, M.; Dietz, H. *Nat. Methods* **2011**, *8*, 221.

(20) Kim, D.-N.; Kilchherr, F.; Dietz, H.; Bathe, M. *Nucleic Acids Res.* **2012**, *40*, 2862.

(21) Chen, H.; Zhang, H.; Pan, J.; Cha, T.-G.; Li, S.; Andréasson, J.; Choi, J. H. *ACS Nano* **2016**, *10*, 4989.

(22) Kuluncsics, Z.; Perdiz, D.; Brulay, E.; Muel, B.; Sage, E. *J. Photochem. Photobiol., B* **1999**, *49*, 71.

(23) Sinha, R. P.; Häder, D.-P. *Photochemical & Photobiological Sciences* **2002**, *1*, 225.

(24) Douki, T.; Sauvaigo, S.; Odin, F.; Cadet, J. *J. Biol. Chem.* **2000**, *275*, 11678.

(25) Jiang, Y.; Ke, C.; Mieczkowski, P. A.; Marszalek, P. E. *Biophys. J.* **2007**, *93*, 1758.

(26) Sancar, A. *Biochemistry* **1994**, *33*, 2.

(27) Chen, H.; Weng, T.-W.; Riccitelli, M. M.; Cui, Y.; Irudayaraj, J.; Choi, J. H. *J. Am. Chem. Soc.* **2014**, *136*, 6995.

(28) Zhou, L.; Marras, A. E.; Su, H.-J.; Castro, C. E. *ACS Nano* **2014**, *8*, 27.

(29) Ke, Y.; Bellot, G.; Voigt, N. V.; Fradkov, E.; Shih, W. M. *Chemical Science* **2012**, *3*, 2587.

(30) Di Pietro, M. L.; Puntoriero, F.; Tuyéras, F.; Ochsenbein, P.; Lainé, P. P.; Campagna, S. *Chem. Commun.* **2010**, *46*, 5169.

DOI: 10.1021/jacs.6b10821
J. Am. Chem. Soc. 2017, 139, 1380–1383